NANO MICRO small

Supporting Information

for *Small,* DOI: 10.1002/smll.202107641

Ion/Electron Redistributed 3D Flexible Host for Achieving Highly Reversible Li Metal Batteries

Huai Jiang, Yangen Zhou, Caohong Guan, Maohui Bai, Furong Qin, Maoyi Yi, Jie Li, Bo Hong, and Yanqing Lai**

Supporting Information

Ion/electron redistributed 3D flexible host for achieving highly reversible Li metal batteries

Huai Jiang, Yangen Zhou, Caohong Guan, Maohui Bai, Furong Qin, Maoyi Yi, Jie Li, Bo Hong, Yanqing Lai**

H. Jiang, Y. Zhou, M. Bai, F. Qin, M. Yi, J. Li, B. Hong, Y. Lai
School of Metallurgy and Environment
Central South University
Changsha 410083, Hunan, China
E-mail: bop_hong@csu.edu.cn, laiyanqing@csu.edu.cn

C. Guan
University of Michigan−Shanghai Jiao Tong University Joint Institute
Shanghai Jiao Tong University
800 Dongchuan Road, Shanghai 200240, China

B. Hong, Y. Lai
Engineering Research Centre of Advanced Battery Materials
The Ministry of Education
Changsha 410083, Hunan, China

Experimental section

1.1. Fabrication of CoP-C@CFC

Preparation of Co-MOF@CFC: The commercial carbon fiber cloth (Hesen Tech Co., Ltd) was treated in concentrated acid of HNO_3/H_2SO_4 (1:3 by volume) before use. Afterward, Co-MOF@CFC precursor was prepared using a solution method. Firstly, 40 mL 2-methylimidazole (0.4 M) and 40 mL $Co(NO_3)_2·6H_2O$ (0.05 M) solutions were prepared, respectively. Then, 2-methylimidazole solution was quickly poured into $Co(NO_3)_2·6H_2O$ solution under vigorous stirring for 5 min. Last, a piece of commercial carbon fiber cloth (5×5

cm) was put into the mixed solution. After 5 h the carbon cloth was taken out, cleaned and dried for further use.

Preparation of Co_3O_4-C@CFC: The Co-MOF@CFC was first annealed in Ar atmosphere at 550 °C for 2 h with a ramp rate of 1 °C min^{-1}, and the temperature was then dropped to 350 °C within 40 min. Then the Ar flow was stopped, the sample was further annealed for 2 h in air at 350 °C and cooled down to room temperature naturally.

Preparation of CoP-C@CFC: For gas-phase phosphorization, 1.2 g NaH_2PO_2 (Sinopharma chemical reagent co., Ltd, China) in a porcelain boat was placed in upstream and a piece of oxidized Co_3O_4-C@CFC was placed in downstream. The annealing temperature was set at 350 °C for 2 h with a ramping rate of 2 °C min^{-1} under an Ar gas flow (OTF-1200X-80SL, KJ GROUP, China). And cooled down to room temperature naturally. The samples were treated at 350 ℃ for 2 h with 2 ℃ min^{-1} under argon gas atmosphere. According to related reports,[1] the involved reactions of CoP-C@CFC preparation were simply expressed as follow:

$$5NaH_2PO_2.6H_2O \xrightarrow{\Delta} Na_4P_2O_7 + NaPO_3 + 2PH_3 + 30H_2O + 2H_2 \quad (1)$$

$$Co_3O_4 + 3PH_3 \xrightarrow{\Delta} 3CoP + 1/2H_2 + 4H_2O \quad (2)$$

1.2. Material characterization

The crystal structure of the samples was characterized by X-ray diffraction (XRD, Empyrean 2, PANalytical). The surface chemical composites were examined using X-ray photoelectron spectroscopy (XPS, Thermo Escalab 250Xi). Scanning electron microscope (SEM, FEI Nova NanoSEM 230) analysis was conducted on a field emission scanning electron microscope at 15 kV. The specific surface area and pore distribution was analyzed by Brunauer-Emmett-Teller (BET, QUADRASORB evo, QUANTACHROME INSTRUMENTS). TEM, high-resolution TEM (HRTEM), selected-area electron diffraction (SEAD) were all performed with a Titan G2 60-300 microscope. In situ optical microscopy (LW300LJT, Beijing CeWei co., Ltd, China) was used to observe Li dendrite growth and volume effect of electrodes.

1.3. Electrochemical performance

CR2032 coin cells with the CoP-C@CFC and CFC as the working electrode and Li foil (Tianjin zhongneng lithium co. Ltd, China) as the counter/reference electrode were assembled in the argon-filled glovebox (Mikrouna (China) co., LTD) for repeated Li deposition/stripping testing. The electrolyte was 1 M LiTFSI in DOL/DME (v/v¼ 1:1) with 2% $LiNO_3$. All the cells were tested using a CT2001A cell test instrument (LAND Electronic Co, China). The

electrochemical impedance spectroscopy (EIS) measurements were performed using a CHI660e electrochemical station (Shanghai Chenhua, China). The EIS measurement was conducted in the frequency range of 0.1 Hz–100 kHz at the reference circuit voltage. For the cycling tests on symmetrical cells, 5 mAh cm^{-2} Li metal was pre-electroplated onto the electrode.

For the full-cell, the $LiFePO_4$ (LFP) was selected and paired with CoP-C@CFC-Li and CFC-Li. The LPF (purchased from BTR, China) was mixed with carbon black and PVDF in a weight ratio of 8:1:1 and then rigorously pasted on an aluminum foil, with areal mass loading of around 3.5 or 5 mg cm^{-2}. Then the mixture was dried at 60 ℃ for 12 h and punched into disks with diameter of 10 mm. Before assemble the full-cell, selected electrode (CoP-C@CFC and CFC) was firstly assembled into a 2032 cell with lithium as counter electrode and deposited with capacity of 5 mAh cm^{-2} at a current density of 0.5 mA cm^{-2}. After deposited with lithium, the cell was disassembled, and the CoP-C@CFC-Li and CFC-Li electrodes were washed with methylcarbonate for several times. Then, the CoP-C@CFC-Li or CFC-Li electrode was pared with the LFP electrode to assemble the full-cell with the electrolyte of 1.0 M $LiPF_6$ in 89 vol% 1:1 w/w ethylene carbonate/diethylcarbonate with 10 vol% fluoroethylene carbonate and 1 vol% vinylenecarbonate. The full-cell was cycled at 0.1 C for initial 3 cycles for activation and SEI formation. The full-cell was galvanostatically cycled between 2.5 and 4.2 V at various rates ranging from 0.2 to 5 C to investigate the electrochemical performance.

1.4. Theoretical calculations

All Spin-polarized first-principle calculations were carried out using Vienna ab initio simulation package (VASP).[2] The exchange-correlation interactions were described by the Perdew–Burke–Ernzerhof (PBE) within the generalized gradient approximation functional (GGA).[3] The dispersion-corrected DFT-D3 method developed by Grimme was utilized to improve weak interactions.[4] The k-point was set to 3×3×1, the corresponding energy cutoff and force tolerance is 450 eV and 0.02 eV $Å^{-1}$, respectively. The graphene (001) with 5×5 supercell and P, Co-doped grapheme (CoP4C) was performed to bond to Li atom. For the pristine grapheme surface, the top (T, above the carbon atom) and hollow sites (H, above the hollow site of six carbon atoms) were considered for Li adsorption. The binding energies (E_b) of Li on different surfaces were calculated using the following equation:[5]

$$E_b = E_{Li/surf} - E_{surf} - E_{Li}$$

where $E_{Li/surf}$, E_{surf} and E_{Li} are the total energy of the Li/surface, the isolated surface and the Li atom, respectively.

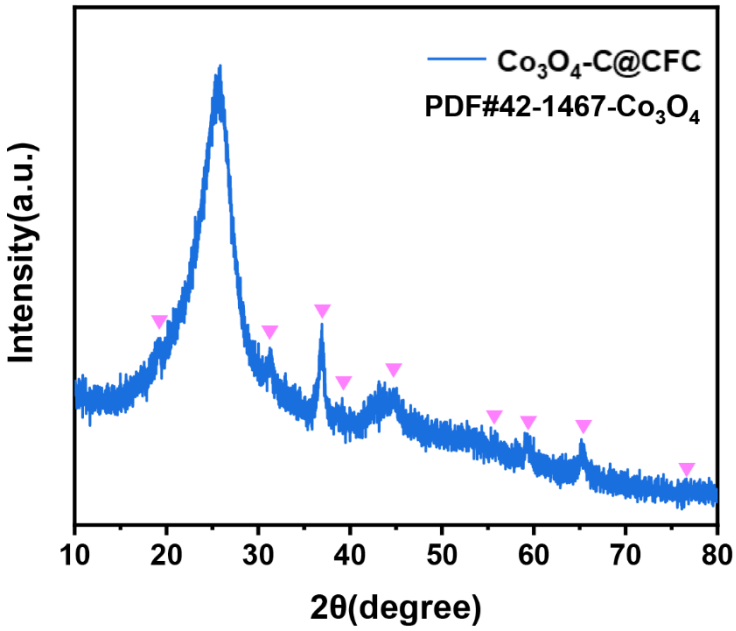

Figure S1. The XRD pattern of Co_3O_4-C@CFC

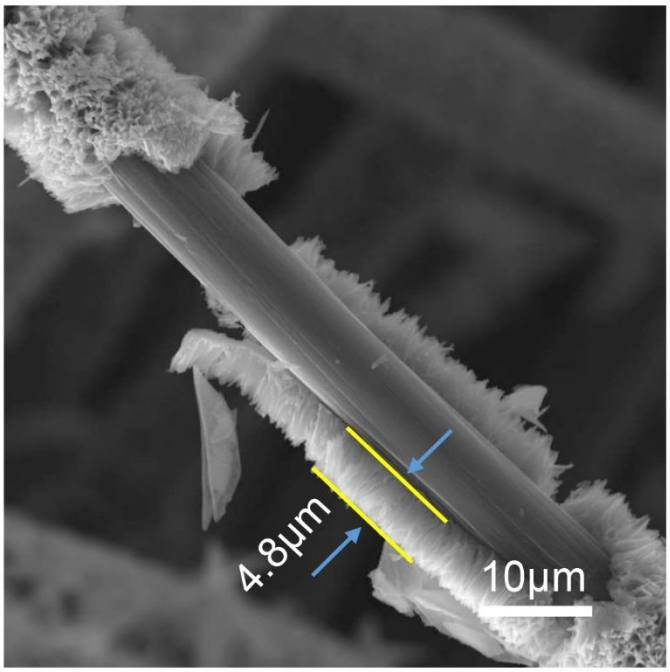

Figure S2. The thickness of CoP sheath on CoP-C@CFC.

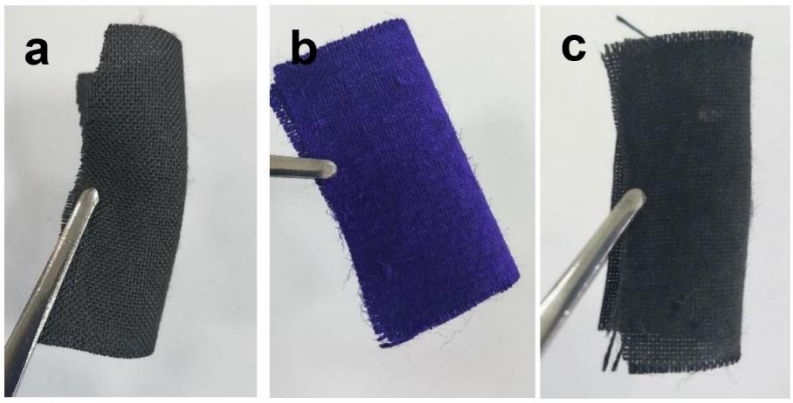

Figure S3. The pictures of the CFC (a), Co-MOF@CFC (b) and CoP-C@CFC (c) with the excellent flexibility.

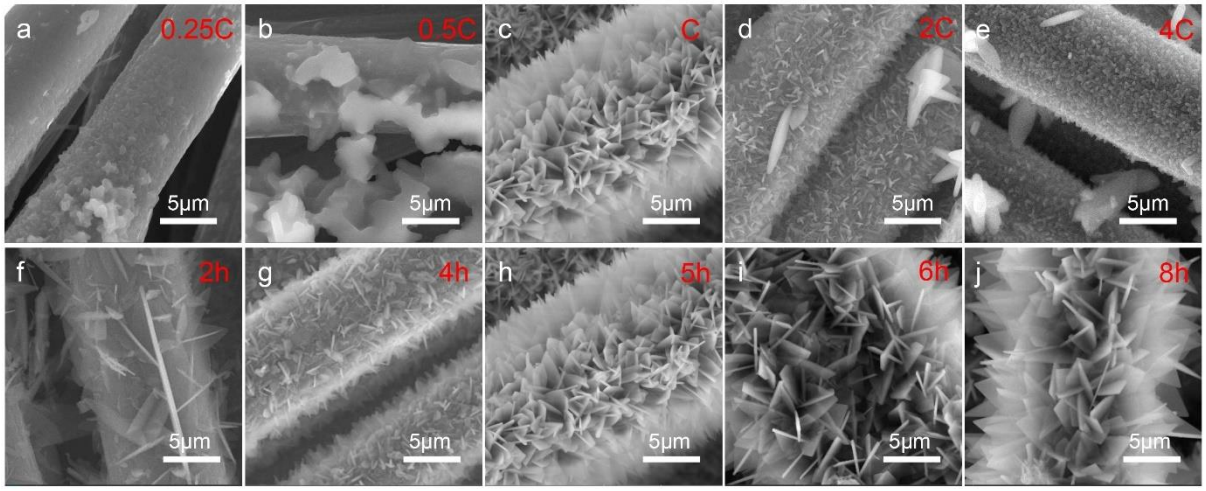

Figure S4. the Co-MOF nanosheets in-situ growth onto CFC under the solution concentration of (a) 0.25C, (b) 0.5C, (c) C, (d) 2C and (e) 4C, 1C is the mixed solution concentration of 0.4 M 2-methylimidazole and 0.05 M $Co(NO_3)_2 \cdot 6H_2O$. the Co-MOF nanosheets in-situ growth onto CFC under the soaking time of (f) 2 h, (g) 4 h, (h) 5 h, (i) 6 h and (j) 8 h.

As shown in Figure S4a-b, when the concentration of the 2-methylimidazole and $Co(NO_3)_2 \cdot 6H_2O$ is halved or diluted down to a quarter, respectively, Co-MOF nanosheets show obvious inhomogeneity. On the contrary, when the concentration of the mixed solution is increased to double (Figure S4d) or quadruple (Figure S4e), Co-MOF nanosheets are smaller and denser. In addition, unattached Co-MOF nanosheets appear due to the excessive concentration of the mixed solution possibly. On other hand, when the CFC is immersed in the mixed solution of 0.4 M 2-methylimidazole and 0.05 M $Co(NO_3)_2 \cdot 6H_2O$ for 2 h (Figure S4f), scattered Co-MOF nanosheets appear on the surface of CFC. With the immerse time raising to 4 h (Figure S4g), relatively even Co-MOF nanosheets in situ grow onto the CFC. The density of Co-MOF nanosheets has no significant change when the immerse time further is increased to 6 h or 8 h (Figure S4i-j).

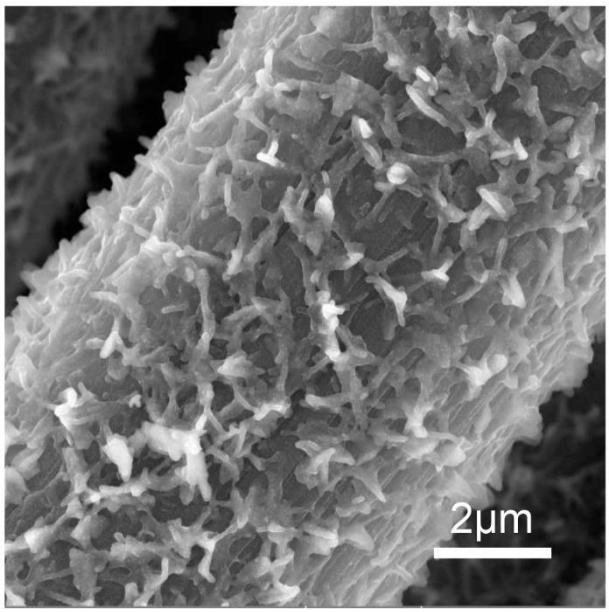

Figure S5. The high magnification SEM images of CoP-C@CFC under the immerse of 4 h.

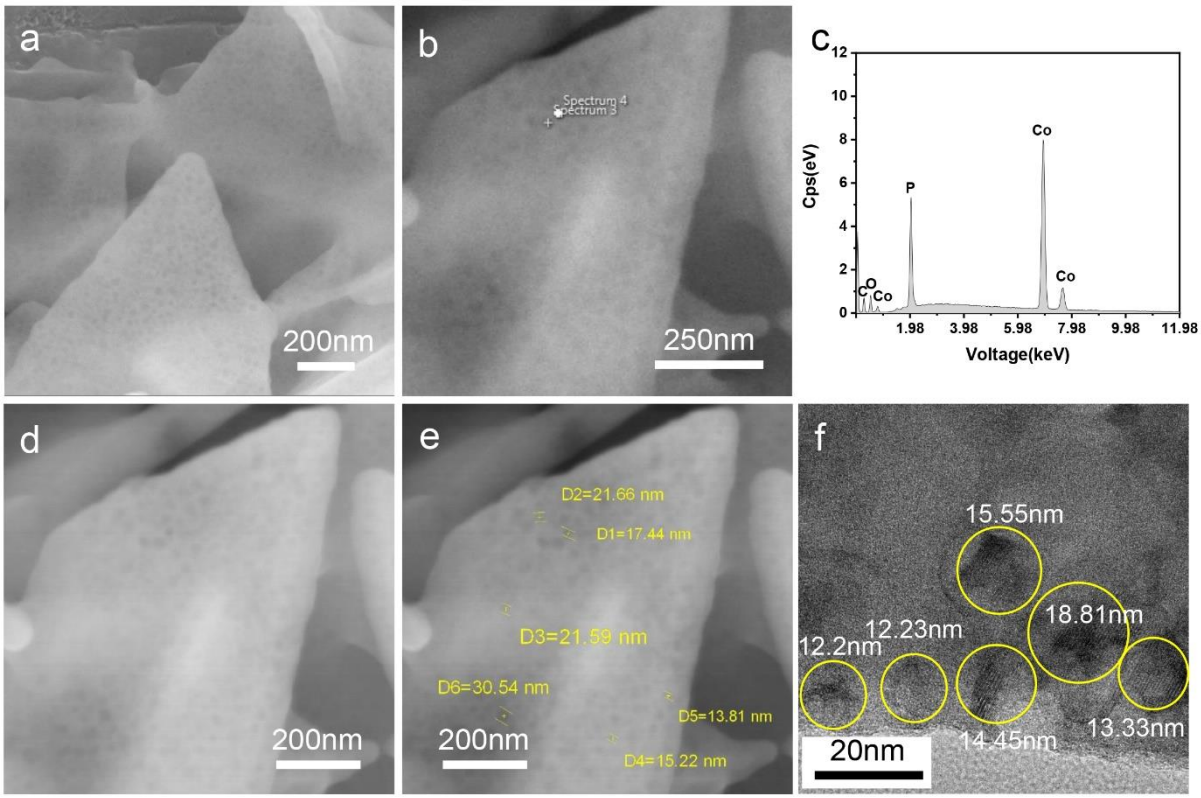

Figure S6. (a) The 200kx high magnification SEM image of CoP nanosheets. The EDX spectrograms (b) and corresponding elements (c) of CoP nanosheets. (d) The 300kx high magnification SEM image of CoP nanosheets. (e) The diameters of the black nanodots on CoP nanosheets. (f) The diameters of CoP nanoparticles in a high magnification TEM image.

As shown in Figure S6a, many black nanodots are uniformly embedded into CoP nanosheets. The black nanodot is tested by EDX spectrograms (Figure S6b), which shows obvious elements of P and Co (Figure S6c). Thus, these black nanodots are testified to be CoP nanoparticles. In 300kx high magnification SEM image of CoP nanosheets (Figure S6d), these CoP nanoparticles appear clearly. The average diameter of CoP nanoparticles is approximately 15 nm by random selection and measurement (Figure S6e). To further testify, a high magnification TEM image of CoP nanosheets is supplied, which presents plenty of about 15 nm nanoparticles with unambiguous lattice fringe of CoP (Figure S6f).

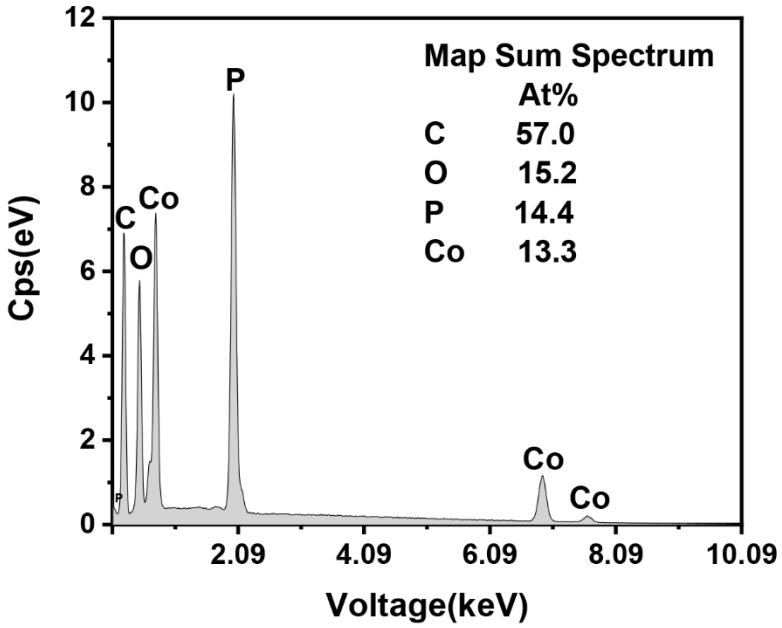

Figure S7. EDX spectrograms of CoP-C@CFC and corresponding atom ratios of C, Co, O and P elementals.

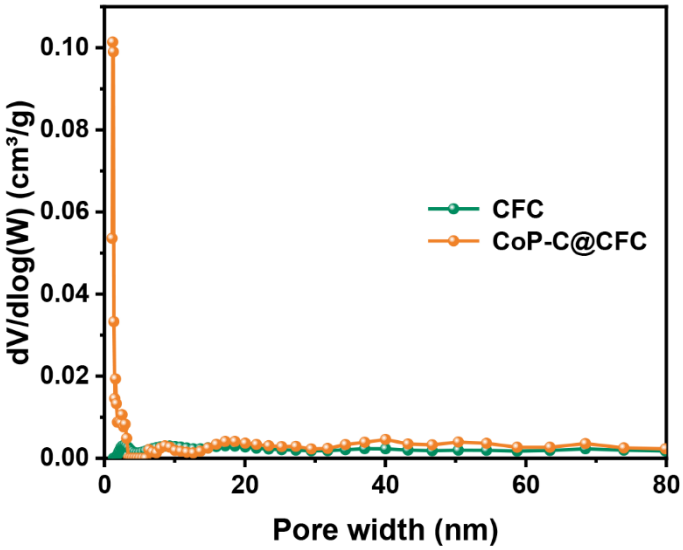

Figure S8. The pore size distribution of CoP-C@CFC.

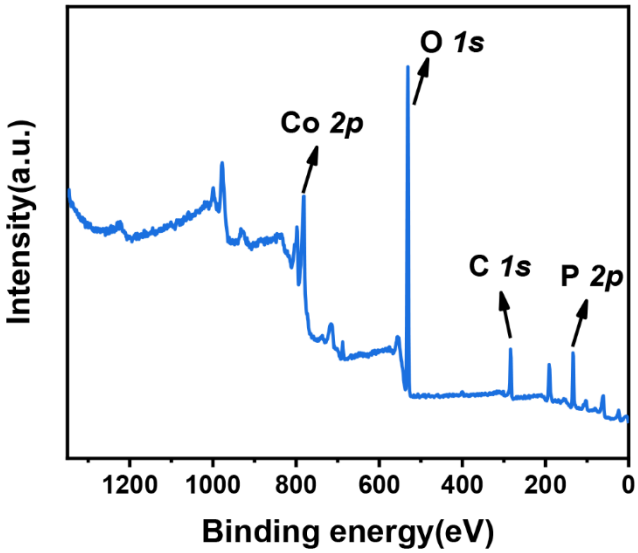

Figure S9. XPS full spectrum of as-synthesized CoP-C@CFC

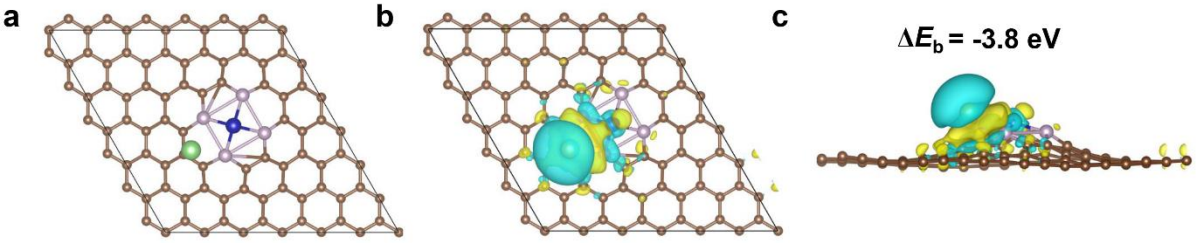

Figure S10. Binding energies of a Li atom with CoP-C@CFC (d) at hollow sites by density functional theory calculations.

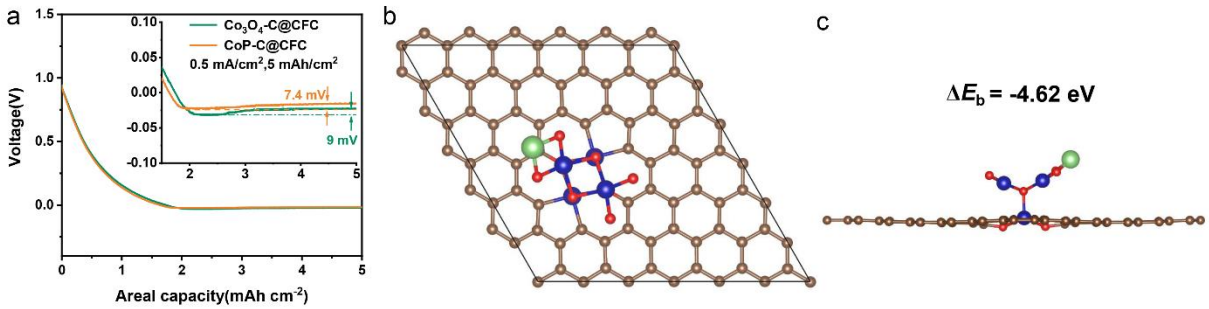

Figure S11. (a) Voltage-capacity curves of Li plating on Co_3O_4-C@CFC and CoP-C@CFC at 0.5 mA cm^{-2}. Adsorption structure of a Li atom on Co_3O_4-C@CFC with a top view (b) and side view (c).

As shown in Figure S11a, the CoP-C@CFC electrode exhibits a lower nucleation overpotential (7.4 mV) compared to the Co_3O_4-C@CFC (9 mV). To further elucidate the result, the binding energy (E_b) of a Li atom with Co_3O_4 in Co_3O_4-C@CFC is estimated by density functional theory (DFT) calculations (Figure S11b-c). Li atom adsorbs on the optimal structure of Co_3O_4-C@CFC,[6,7] which displays the calculated binding energy (ΔE_b) of -4.62 eV. Comparatively, the calculated binding energy of Li atom with CoP-C@CFC is -6.4 eV, which confirms superior Li affinity relative to Co_3O_4-C@CFC.

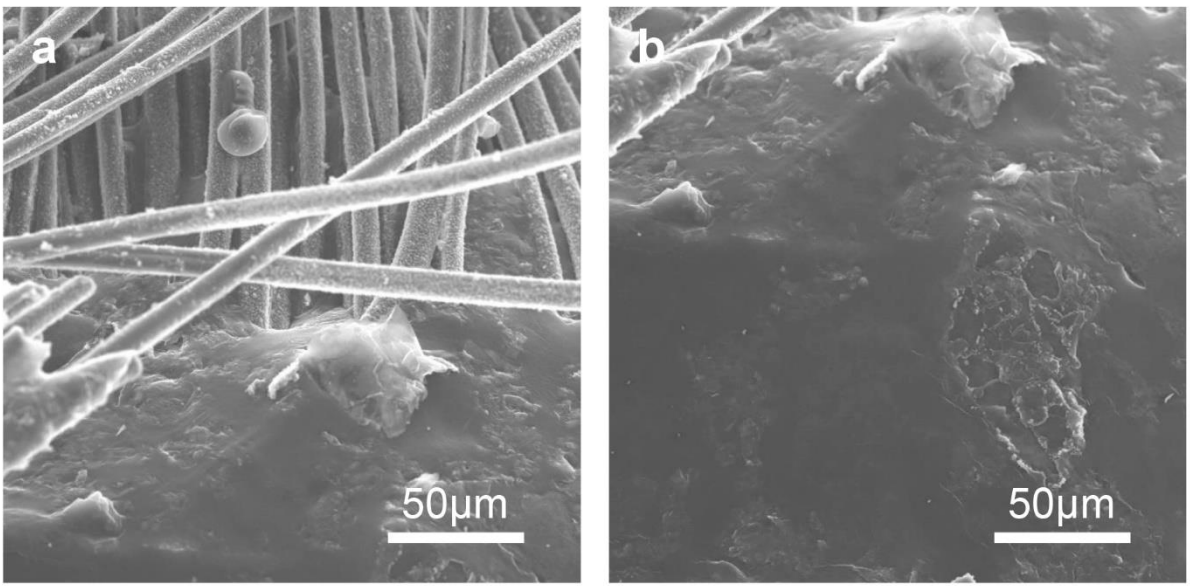

Figure S12. SEM images of molten Li spreading (a) and covered (b) on CoP-C@CFC.

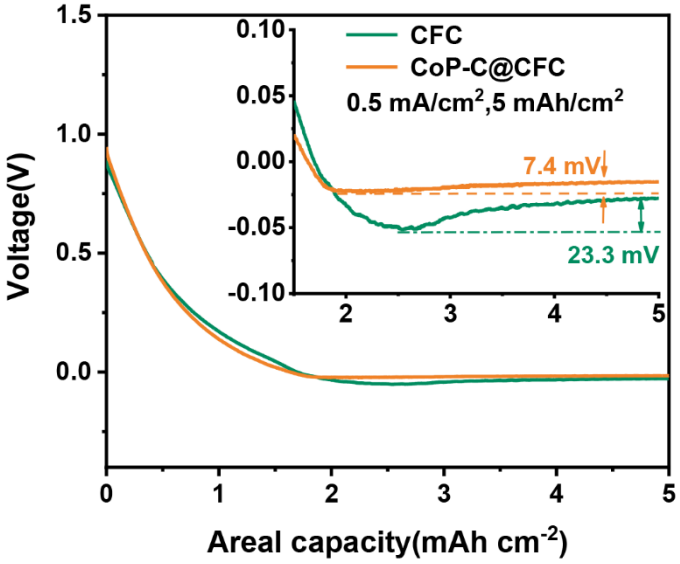

Figure S13. Voltage-capacity curves of Li plating on bare CFC and CoP-C@CFC at 0.5 mA cm^{-2}.

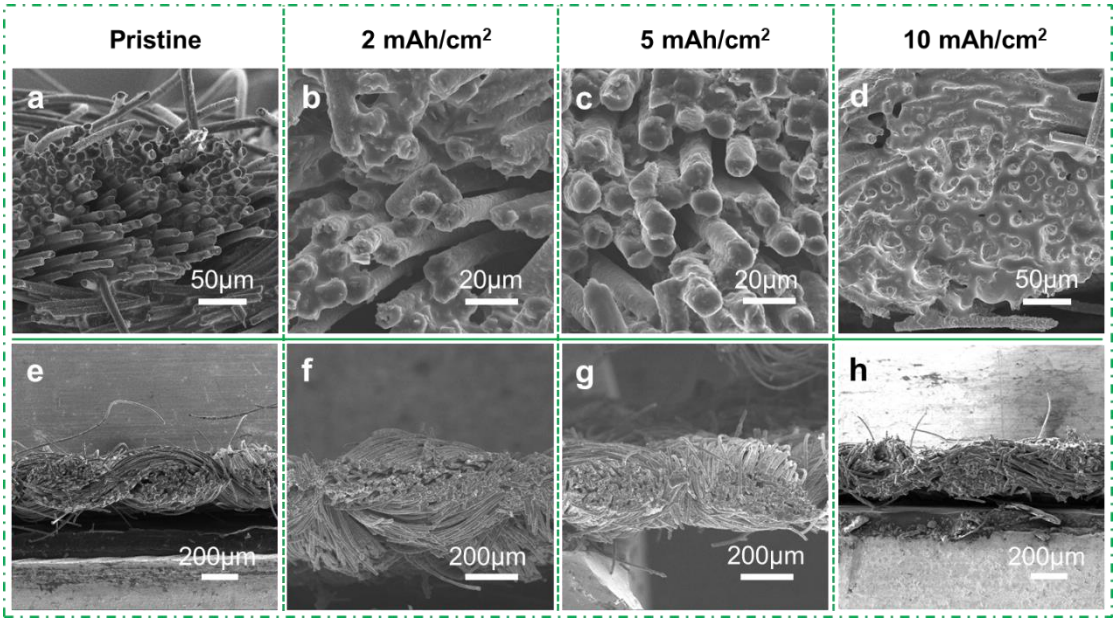

Figure S14. Cross-section SEM images of CoP-C@CFC electrode with 0 (a, e), 2 (b, f), 5 (c, g) and 10 mAh cm^{-2} (d, h), respectively.

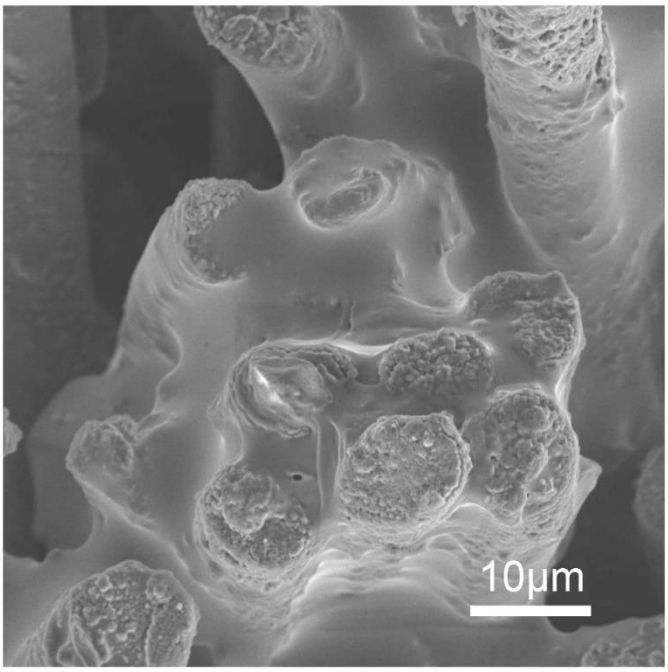

Figure S15. The high magnification SEM images of CoP-C@CFC deposited with the capacity of 10 mAh cm^{-2}.

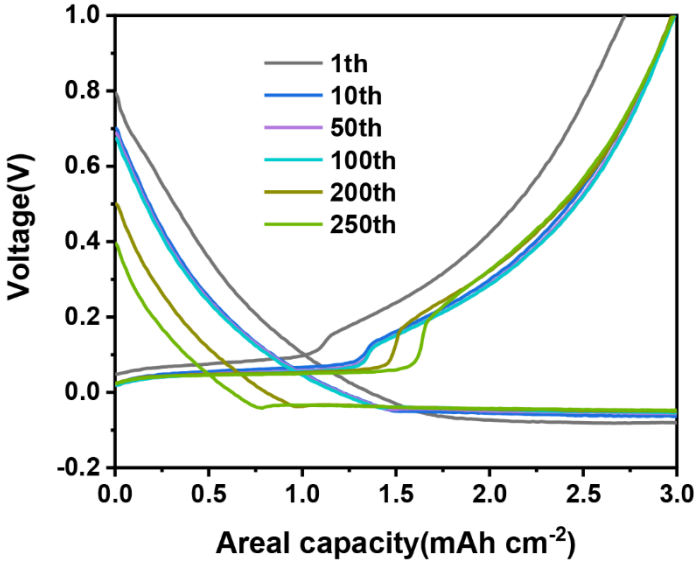

Figure S16. Voltage-capacity profiles for CoP-C@CFC at 5 mA cm^{-2} with a total capacity of 3 mAh cm^{-2}.

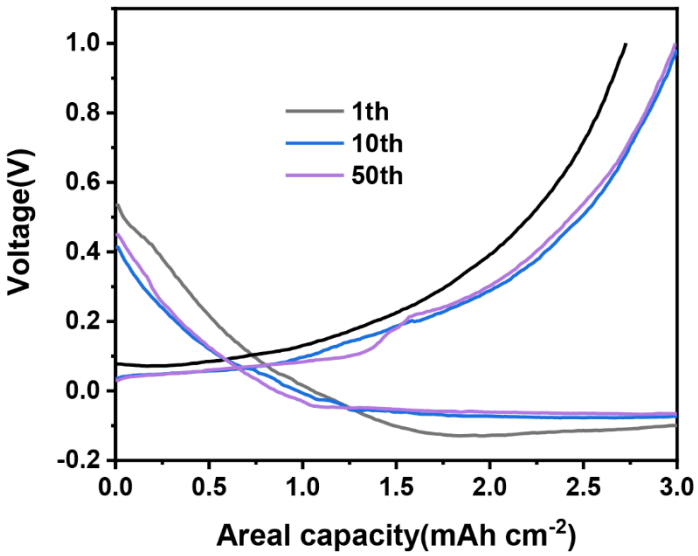

Figure S17. Voltage-capacity profiles for CFC at 5 mA/cm^2 with a total capacity of 3 mAh/cm^2.

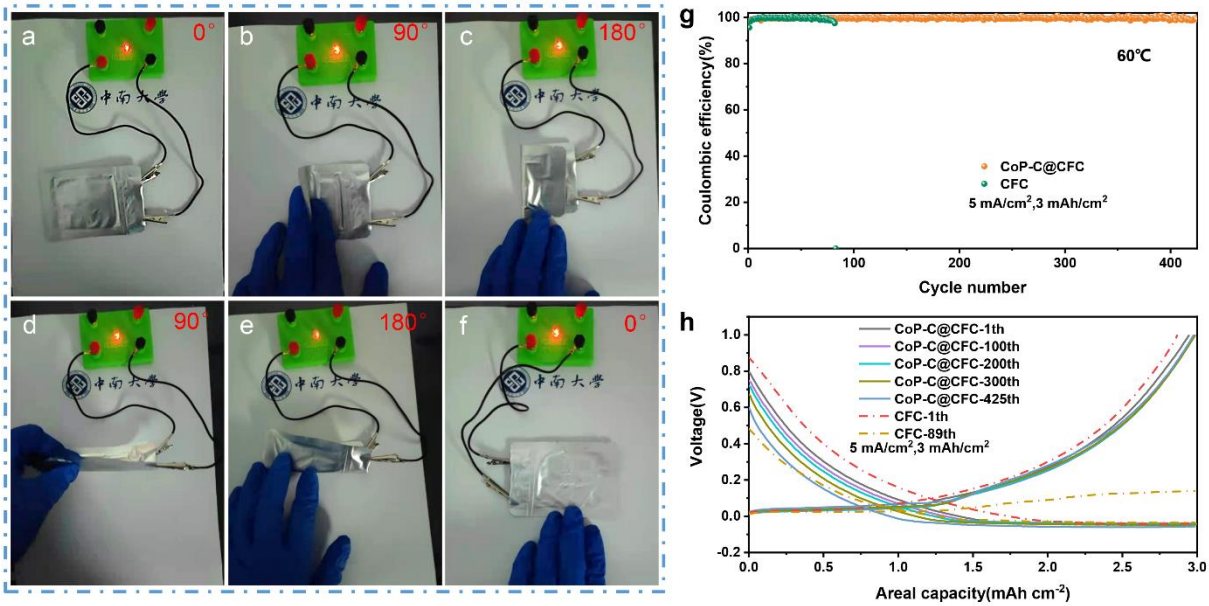

Figure S18. (a-f) Qualitative demonstration of the stability of the 3D carbon fiber cloth on the folding processes of Li||CoP-C@CFC pouch cell by checking the LED illumination. The coulombic efficiencies (g) and voltage-capacity curves (h) of CoP-C@CFC under 60℃ during the charging/discharging of the batteries.

As shown in Figure S18(a-f), the light-emitting diode (LED) could be lighted under the 2.5 V Li||CoP-C@CFC pouch cell (Figure S18a). And then, the pouch cell is curved vertically by 90° (Figure S18b) and 180° (Figure S18c), respectively. Subsequently, when the pouch cell is folded horizontally by 90° (Figure S18d) and 180° (Figure S18e), respectively, there is still no noticeable change in the lighting intensity of the LED. In end, the pouch cell is recovered flat (Figure S18f), the LED still maintains the light. Additionally, when the test temperature is increased to 60℃, the coin half-cell with CoP-C@CFC electrode can keep 425 cycles with a high average Coulombic efficiency (CE) 99.2% at 5 mA cm^{-2} with a total capacity of 3 mAh cm^{-2} (Figure S18g). Moreover, stable Li plating/stripping can be achieved, which is reflected in voltage-capacity curves (Figure S18h). Comparatively, CFC shows a low CE of 97.45% after 80 cycles and goes down to zero very quickly due to short circuit.

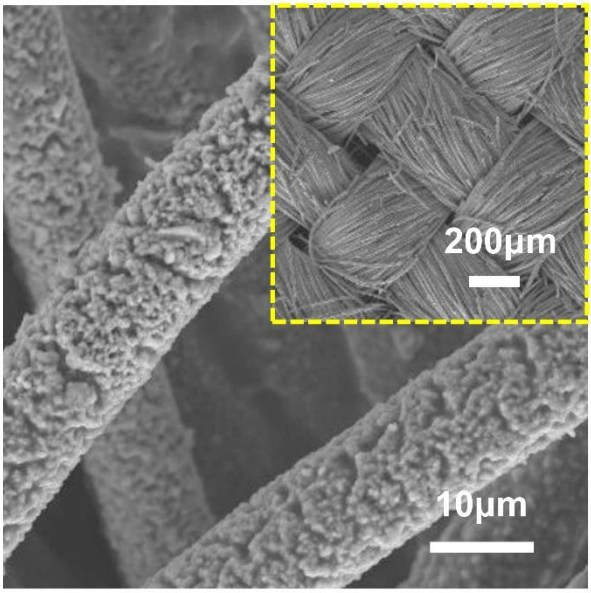

Figure S19. SEM images of CoP-C@CFC electrode stripped with 2 mAh cm^{-2} cycled after 50 cycles at 2 mA cm^{-2}.

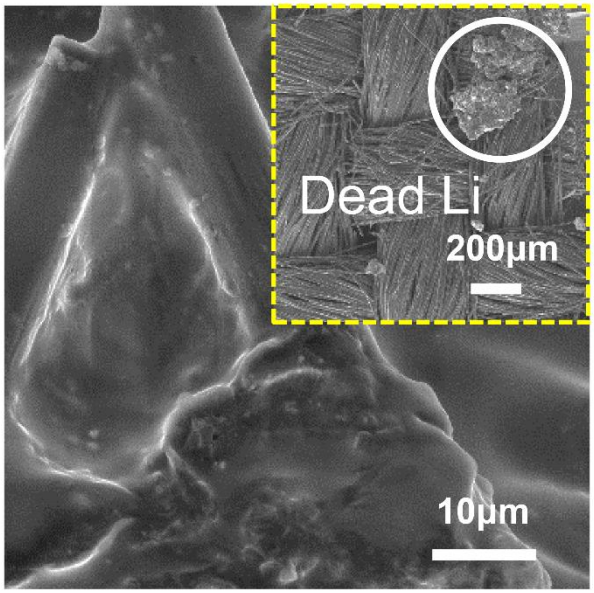

Figure S20. SEM images of CFC electrode stripped with 2 mAh cm^{-2} cycled after 50 cycles at 2 mA cm^{-2}.

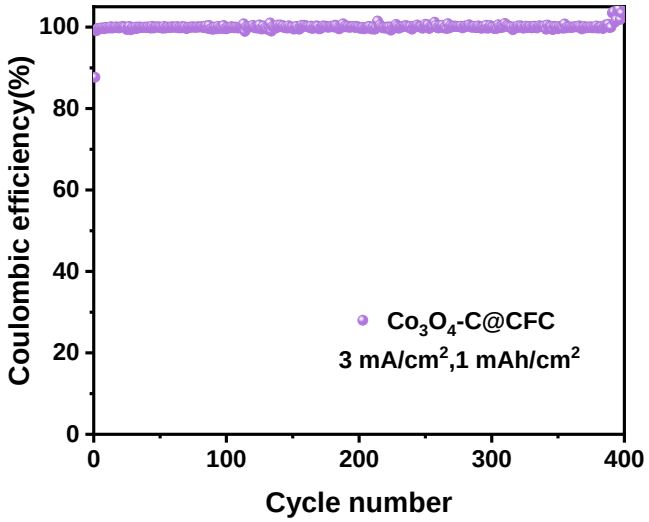

Figure S21. Coulombic efficiency of Co_3O_4-C@CFC at 3 mA cm^{-2} with a total capacity of 1 mAh cm^{-2}.

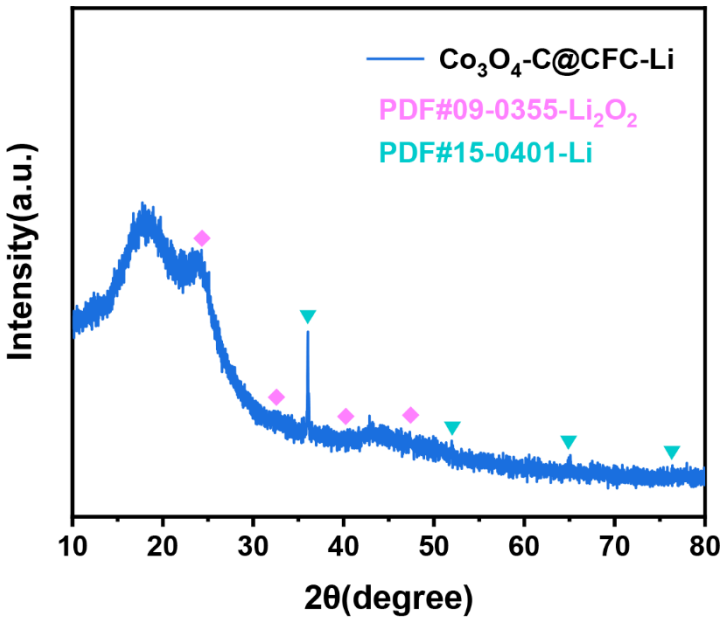

Figure S22. XRD patterns of Co_3O_4-C@CFC composited with Li metal.

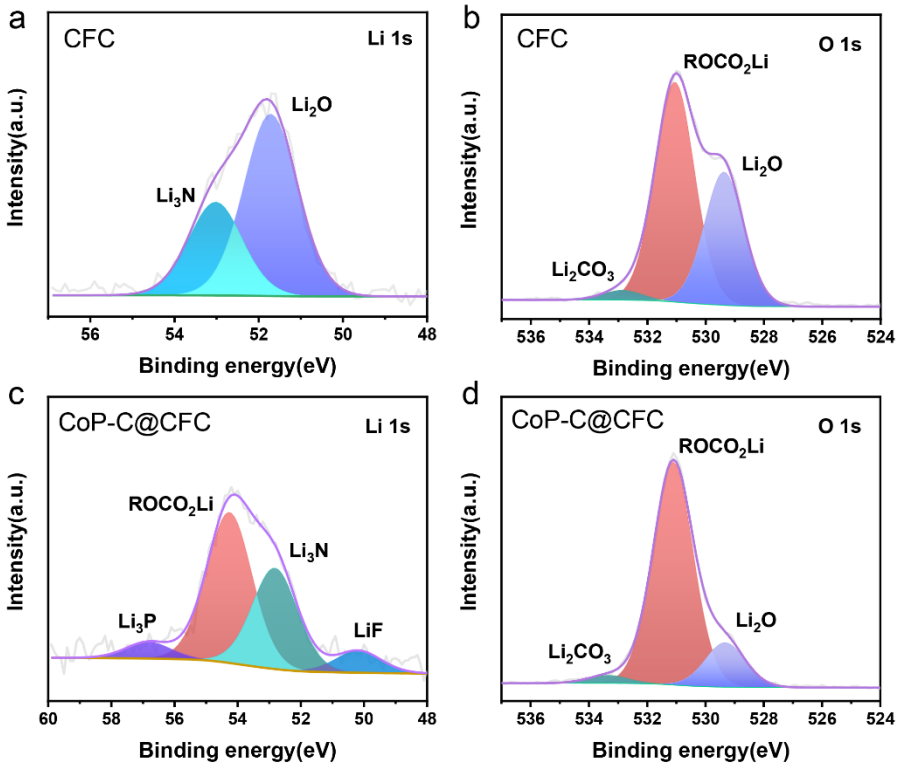

Figure S23. High-resolution XPS analysis of the (a) Li 1s, (b) O 1s peaks obtained from SEI films of CFC. High-resolution XPS analysis of the (c) Li 1s, (d) O 1s peaks obtained from SEI films of CoP-C@CFC. The electrodes run 50 cycles at the current density of 2 mA cm^{-2} with the capacity of 2 mAh cm^{-2} in the half cell.

As shown in Figure S23(a-b), the SEI composition of CFC is mainly composed of inorganic Li_3N,[8] Li_2O,[9-11] Li_2CO_3 as well as organic $ROCO_2Li$. It indicates the SEI of CFC is consistent with a typical multilayer SEI model, which is composed of the inorganic-rich inner and organic-rich outer SEI layers.[12] Furthermore, because the SEI on CFC is an irregular mosaic SEI structure and randomly disperses organic and inorganic grains, SEIs of this type lack flexibility, making them vulnerable during interfacial fluctuation.[13] Even, a mass of dead Li and excess SEI are accumulated on the CFC electrode after repeated plating/stripping process (Figure S20), which is further testified by increased interfacial transfer impedance of CFC electrode (Fig. 6g). Comparatively, the Li_3P,[14] Li_3N, LiF[15] counts, and weaker Li_2O can be observed in the SEI of CoP-C@CFC (Figure S23(c-d)), which indicates the early formed SEI on CoP-C@CFC effectively inhibits further electrolyte decomposition. Perhaps the signal of Li_2O in O 1s is caused by oxidation due to unavoidable exposure of the sample.[16] Meanwhile, Li_3P and LiF-rich SEI induced by CoP[17] and LiTFSI,[18] respectively, which is uniform and conductive for Li-ion diffusion,[19-20] realizing smooth and dense Li deposits, high Coulombic efficiency, and reducing the formation of dead Li (Figure S19).

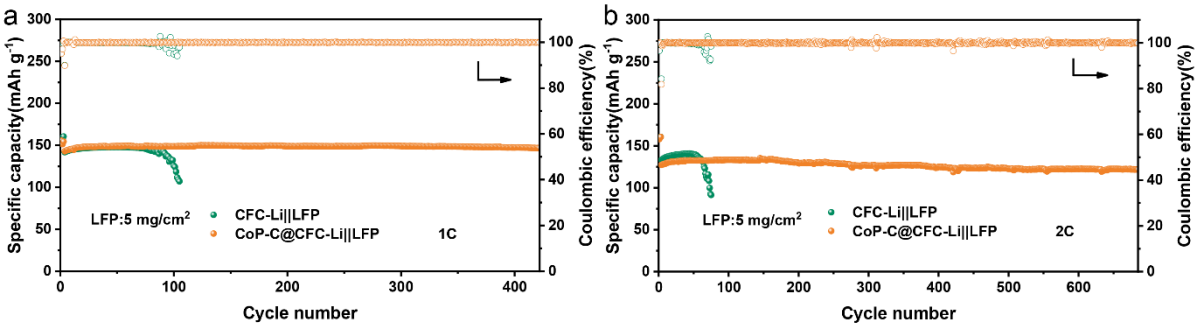

Figure S24. Cycling performance of full cell at 1 C (a) and 2 C (b) with the cathode loading of 5 mg cm^{-2}.

The $LiFePO_4$ (LFP) electrodes were prepared under laboratory conditions, whose active loading was maximally increased to 5 mg cm^{-2}. Assembled with CoP-C@CFC-Li anode of 5 mAh cm^{-2}, the full cell keeps the discharge capacity of 147 mAh g^{-1} with a stable CE of 99.92% at 1 C after 422 cycles (Figure S24a). The capacity retention ratio is 98%. By contrast, the full cell of CFC-Li||LFP only runs 90 cycles with rapid capacity attenuation. Even if the current density is increased to 2 C (Figure S24b), the full cell of CoP-C@CFC-Li||LFP still holds the discharge capacity of 122 mAh g^{-1} with a stable CE of 99.9% after 685 cycles. Moreover, the capacity retention ratio is up to 91.7%. However, the full cell of CFC-Li||LFP shows obvious battery failure only after 70 cycles. Therefore, the host of CoP-C@CFC can bear higher cathode loading and exhibit potential application.

References

[1] Z. Wang, J. Shen, J. Liu, X. Xu, Z. Liu, R. Hu, L. Yang, Y. Feng, J. Liu, Z. Shi, L. Ouyang, Y. Yu, M. Zhu, Adv. mater. **2019**, *31*, e1902228.

[2] G. Kresse and J. Furthmuller, Phys. Rev. B: Condens. Matter Mater. Phys. **1996**, *54*, 11169.

[3] K. B. John P. Perdew, Matthias Ernzerhof, Phys. Rev. Lett. **1996**, *77*, 3865.

[4] K. Lee, É. D. Murray, L. Kong, B. I. Lundqvist, D. C. Langreth, Phys. Rev. B **2010**, *82*, 081101.

[5] H. Valencia, A. Gil, G. Frapper, J. Phys. Chem. C **2010**, *114*, 14141.

[6] G. Zhuang, Y. Gao, X. Zhou, X. Tao, J. Luo, Y. Gao, Y. Yan, P. Gao, X. Zhong, J. Wang, *Chem. Eng. J.* **2017**, *330*, 1255.

[7] B. Liu, W. Song, H. Wu, Z. Liu, Y. Teng, Y. Sun, Y. Xu, H. Zheng, *Chem. Eng. J.* **2020**, *398*, 125498.

[8] D. Luo, L. Zheng, Z. Zhang, M. Li, Z. Chen, R. Cui, Y. Shen, G. Li, R. Feng, S. Zhang, G. Jiang, L. Chen, A. Yu, X. Wang, *Nat. Commun.* **2021**, *12*, 186.

[9] Y. Wang, F. Liu, G. Fan, X. Qiu, J. Liu, Z. Yan, K. Zhang, F. Cheng, J. Chen, *J. Am. Chem. Soc.* **2021**, *143*, 2829.

[10] Q. Liu, Y. Xu, J. Wang, B. Zhao, Z. Li, H. B. Wu, *Nano-Micro Lett.* **2020**, *12*, 176.

[11] Q. Zhao, Y. Deng, N. W. Utomo, J. Zheng, P. Biswal, J. Yin, L. A. Archer, *Nat. Commun.* **2021**, *12*, 6034.

[12] H. Kwon, J. Lee, Y. Roh, J. Baek, D. J. Shin, J. K. Yoon, H. J. Ha, J. Y. Kim, H. Kim, *Nat. Commun.* **2021**, *12*, 5537.

[13] D. Lin, Y. Liu, Y. Cui, *Nat. Nanotechnol.* **2017**, *12*, 194.

[14] Z. Luo, S. Li, L. Yang, Y. Tian, L. Xu, G. Zou, H. Hou, W. Wei, L. Chen, X. Ji, *Nano Energy* **2021**, *87*, 106212.

[15] https://srdata.nist.gov/xps/EngElmSrchQuery.aspx?EType=PE&CSOpt=Retri_ex_dat &Elm=Li

[16] L. Lin, F. Liang, K. Zhang, H. Mao, J. Yang, Y. Qian, *J. Mater. Chem. A* **2018**, *6*, 15859.

[17] C. Fu, S. Lin, C. Zhao, J. Wang, L. Wang, J. L. Bao, Y. Wang, T. Liu, *Energy Storage Mater.* **2022**, 45, 1109.

[18] Y. Liu, X. Tao, Y. Wang, C. Jiang, C. Ma, O. Sheng, G. Lu, X. Lou, *Science* **2022**, *375*, 739.

[19] X. Zhang, X. Cheng, X. Chen, C. Yan, Q. Zhang, *Adv. Funct. Mater.* **2017**, *27*, 1605989.

[20] C. Sun, A. Lin, W. Li, J. Jin, Y. Sun, J. Yang, Z. Wen, *Adv. Energy Mater.* **2019**,

1902989.